01 Jan 2023

Development, Validation And Implementation Of Multiple Radioactive Particle Tracking Technique

Mehul S. Vesvikar

Thaar M. Aljuwaya

Mahmoud M. Taha

Muthanna H. Al-Dahhan
Missouri University of Science and Technology, aldahhanm@mst.edu

Recommended Citation

M. S. Vesvikar et al., "Development, Validation And Implementation Of Multiple Radioactive Particle Tracking Technique," *Nuclear Engineering and Technology*, Elsevier, Jan 2023.
The definitive version is available at https://doi.org/10.1016/j.net.2023.07.043

Nuclear Engineering and Technology xxx (xxxx) xxx

Contents lists available at ScienceDirect

Nuclear Engineering and Technology

journal homepage: www.elsevier.com/locate/net

Original Article

Development, validation and implementation of multiple radioactive particle tracking technique

Mehul S. Vesvikar [a,b], Thaar M. Aljuwaya [c,d,*], Mahmoud M. Taha [e], Muthanna H. Al-Dahhan [c,f,g,**]

[a] BIOMATH, Dept of Applied Mathematics, Biometrics and Process Control, Ghent University, Gent, Belgium
[b] Chemical Reaction Engineering Laboratory, Department of Chemical Engineering, Campus Box 1198, 1 Brookings Drive, Washington University, St. Louis, MO, 63130-4899, USA
[c] Nuclear Engineering and Radiation Science Department, Missouri University of Science and Technology (Missouri S&T), Rolla, MO, 65409, USA
[d] Nuclear Technologies Institute, King Abdulaziz City for Science and Technology (KACST), P.O. Box 6086, Riyadh, 11442, Saudi Arabia
[e] College of Engineering and Technology, American University of the Middle East, Kuwait
[f] Multiphase Flows and Reactors Engineering and Education Laboratory (mFReel), Chemical and Biochemical Engineering Department, Missouri University of Science and Technology (Missouri S&T), Rolla, MO, 65409, USA
[g] TechCell, Mohammed VI Polytechnic University, Hay Moulay Rachid 43150, Ben Guerir, Morocco

ARTICLE INFO

Keywords:
Multiple radioactive particle tracking technique
Three phase slurry bubble column
Flow pattern
Hydrodynamics
Non-invasive

ABSTRACT

Computer Automated Radioactive Particle Tracking (CARPT) technique has been successfully utilized to measure the velocity profiles and mixing parameters in different multiphase flow systems where a single radioactive tracer is used to track the tagged phase. However, many industrial processes use a wide range of particles with different physical properties where solid particles could vary in size, shape and density. For application in such systems, the capability of current single tracer CARPT can be advanced to track more than one particle simultaneously. Tracking multiple particles will thus enable to track the motion of particles of different size shape and density, determine segregation of particles and probing particle interactions. In this work, a newly developed Multiple Radioactive Particle Tracking technique (M-RPT) used to track two different radioactive tracers is demonstrated. The M-RPT electronics was developed that can differentiate between gamma counts obtained from the different radioactive tracers on the basis of their gamma energy peak. The M-RPT technique was validated by tracking two stationary and moving particles (Sc-46 and Co-60) simultaneously. Finally, M-RPT was successfully implemented to track two phases, solid and liquid, simultaneously in three phase slurry bubble column reactors.

1. Introduction

Radioactive isotopes, in the form of radiotracers, have been widely used in research and development and industries for monitoring, control, troubleshooting, inspection, optimization and numerous other purposes [1–3]. Radiotracers are widely used in various industrial applications where it can be utilized to monitor and analyze various industrial processes. The use of radiotracers allows for real-time monitoring and tracking of industrial processes, enabling operators to optimize their performance and efficiency. One of the primary applications of radiotracers in industry is in the oil and gas sector. Radiotracers are used to monitor oil reservoirs and to track the movement of oil and gas through pipelines. By injecting radiotracers into the reservoir, operators can track the flow of oil and gas, identify blockages and leaks, and optimize production. Radiotracers also have proven to be a valuable tool in advancing and benchmarking the hydrodynamics of nuclear systems in laboratory settings [4,5] and manufacturing process of TRISO particle [6–8]. Radiotracers are also used in the chemical industry to monitor the flow of chemicals through reactors and to optimize reaction conditions. By monitoring the movement of radiotracers

* Corresponding author. Nuclear Engineering and Radiation Science Department, Missouri University of Science and Technology (Missouri S&T), Rolla, MO, 65409, USA.
** Corresponding author. Nuclear Engineering and Radiation Science Department, Missouri University of Science and Technology (Missouri S&T), Rolla, MO, 65409, USA.
E-mail addresses: taljuwaya@kacst.edu.sa (T.M. Aljuwaya), aldahhanm@mst.edu (M.H. Al-Dahhan).

https://doi.org/10.1016/j.net.2023.07.043
Received 9 November 2022; Received in revised form 15 July 2023; Accepted 31 July 2023

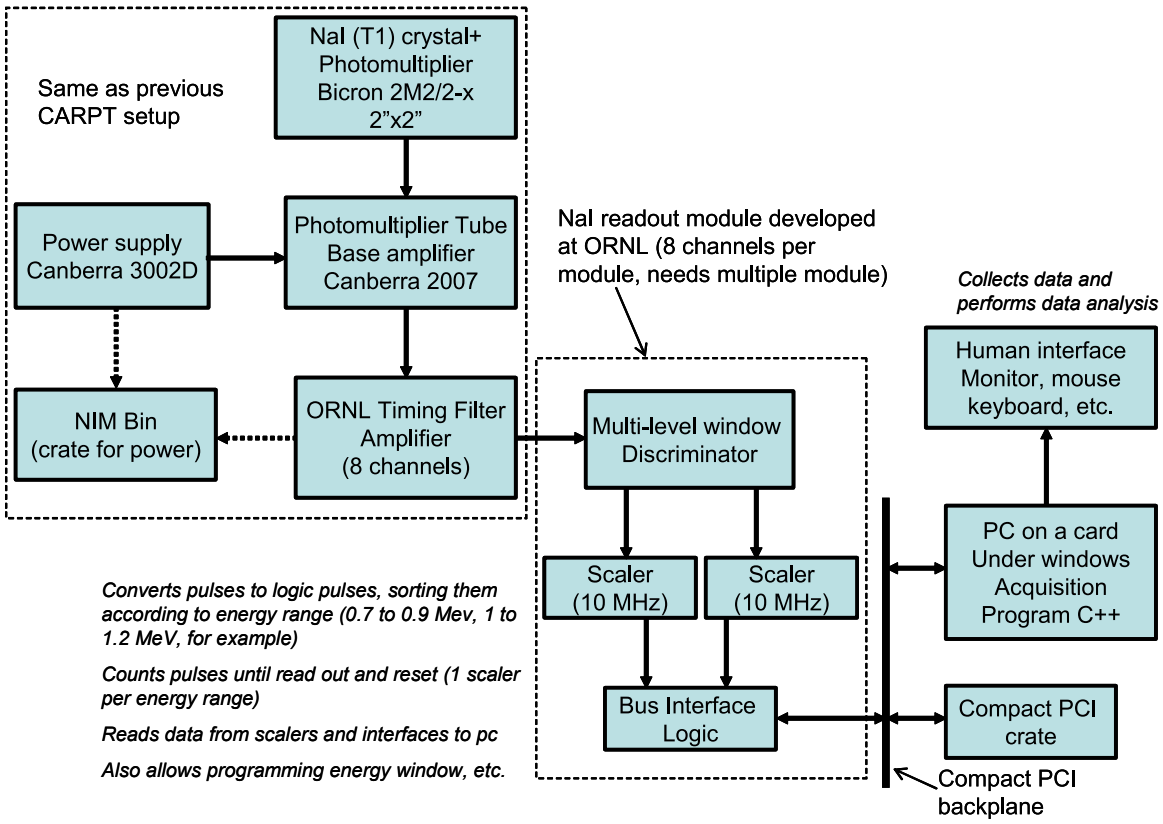

Fig. 1. Schematic diagram of the electronics used in the Multiple radioactive particles tracking (M-RPT) techniques.

through the reactor, operators can track the progress of the reaction and adjust conditions to achieve the desired product yield and quality. Radiotracers are also used in the mining industry to track the movement of minerals through processing plants. By injecting radiotracers into the mineral concentrate, operators can track its movement through the plant, identify inefficiencies, optimize the process, and improve the quality of the final product. In industrial practice, radioisotope-based measurement techniques are most appropriate for monitoring multiphase flow systems, as these systems are opaque and consist of dispersed phases. Such measurement techniques offer a quick and accurate means of monitoring the flow rate of each phase, providing valuable data for process optimization. These techniques are also well-suited for monitoring processes in which multiple phases are present, as the radioisotope can be used to distinguish between the different phases. Multiphase flow systems involve two or more phases (gas, liquid, solid) simultaneously interacting in various forms. Multiphase flow systems have found widespread applications in a broad range of processes, including nuclear, chemical, petroleum, gas processing, biochemical, environmental and mineral processes. For example, multiphase systems are used in oil and gas production, where oil, natural gas and water flow through the same pipe simultaneously. In addition, multiphase flow systems can be used in areas such as combustion, heat transfer, fluidized beds, and others, making them an invaluable tool in many industries. In transparent systems, multiple techniques are being used to visualize the flow of the system and measure the parameters quantitatively such as Particle Image Velocimetry (PIV), Laser Doppler Anemometry (LDA), Planar Laser-Induced Fluorescence (PLIF), and Digital Image Correlation (DIC). However, high energy gamma ray photons-based measurement techniques are needed to study the phase distributions and mixing in opaque multiphase systems. To understand opaque systems in greater detail, powerful gamma ray sources and detectors can be employed to measure the gamma ray intensity, which in turn can provide valuable insight into the system's flow dynamics. Various radioactive isotope-based techniques have been developed for laboratory and site applications in different industrial processes to monitor multiphase systems flow [9–13]. Among several radioisotope-based measurement techniques reported in literature, the computer automated radioactive particle tracking (CARPT) technique has demonstrated capability to picture out flow fields of multiphase flow systems. The CARPT technique offers a unique and valuable insight into the behavior of multiphase flow systems, providing detailed information on their internal flows that other techniques are unable to provide. The CARPT technique has been successfully used to map flow fields and mixing in various opaque single phase and multiphase systems using a single radioactive tracer particle. This technique relies on the use of a radioactive particle that is injected into the system and tracked as it moves through the system. By tracking the particle's movements, it can be accurately map out the flow field and study the internal dynamics of the system. This is a very powerful tool that can provide valuable insights into the behavior of the system that would be difficult to obtain with other techniques. The CARPT technique has been successfully to map flow fields and mixing in various opaque single phase and multiphase systems using a single radioactive tracer particle. It has been applied to study hydrodynamics of gas-liquid bubble columns [14–16], fixed beds under incipient fluidization [17], slurry bubble columns [18], gas-liquid-solid ebulated beds [19], liquid solid riser [20], gas-solids fluidized beds [21], gas-solids spouted beds [6–8], stirred tanks [22,23], algae photobioreactor [24–27] and anaerobic digester [28,29]. In the CARPT technique, a single radioactive particle is used in the reactors to track the tagged phase by means of collimated or non-collimated array of detectors. This array of detectors records number of counts and give information about instantaneous positions of tracer particle after analyzing the data. Time derivatives of instantaneous positions data provide instantaneous velocity components for tracer trajectories. In certain reactor types where slow flow zones or dead zones are present, CARPT suffers from slower data collection rates and sometimes halts due to solids settling. These problems are

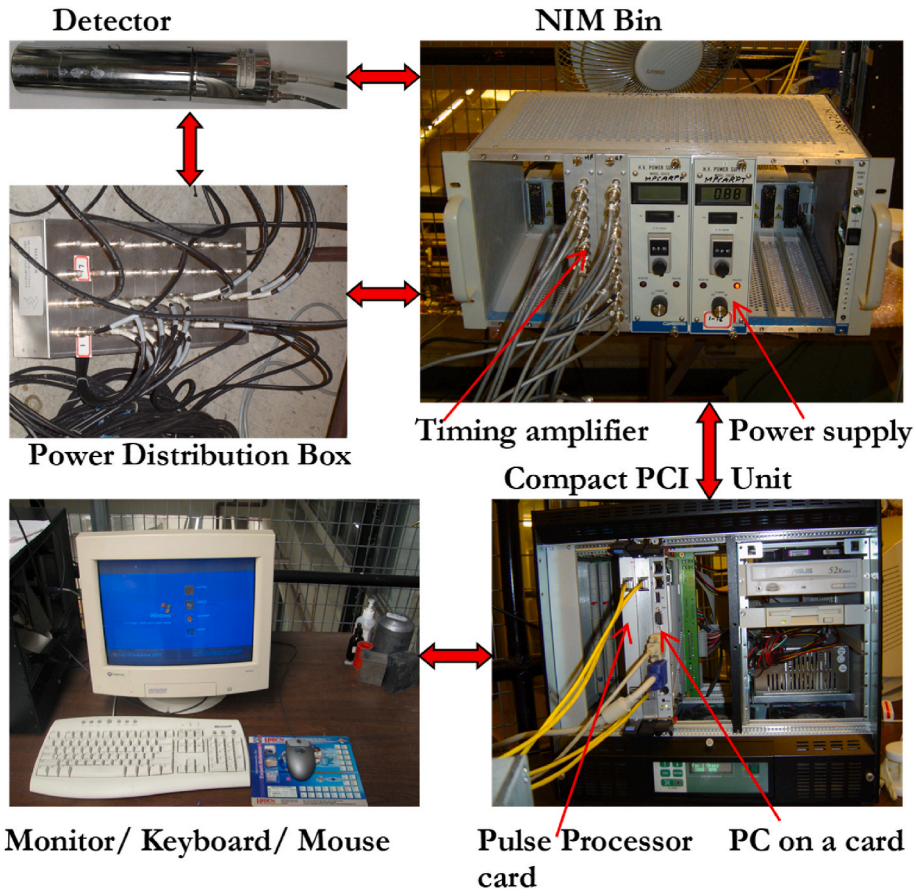

Fig. 2. M-RPT electronics components and connections.

exacerbated by an increase in operation scale. In addition, a number of important multiphase reactors consist of particles having different properties (size, shape, and density), such as binary solids spouted bed [8,30,31] and binary solids fluidized beds [32–34], while the CARPT technique uses only a single tracer particle. Thus, all the required information such as the hydrodynamic behavior of solids of different physical properties, and the segregation and interaction of solid particles could not be obtained by tracking a single radioactive particle. These drawbacks and limitations of CARPT can be overcome by introducing multiple tracer particles that can be tracked simultaneously and this is the prime motivation for the presented study.

In the literature, since the introduction of the RPT in 1985 by Ref. [35] different studies have been conducted towards the development, source selection, optimization, reconstruction methods of the CARPT technique [36–48]. However, among the reported studies, only one study has been reported about the introducing of multiple tracer particles into the CARPT [43]. Accordingly, the objective of this work is to provides evidence that multiple tracer particles can be effectively introduced into the CARPT to obtain more accurate results. By introducing radioactive particles emitting distinct energies of gamma radiation and are of different isotopes, multiple radioactive particles (M-RPT) can be performed [43]. With the use of advanced technology, new assemblies can also be made compact, cheaper, faster, more efficient, and user-friendly. The M-RPT technique will be a valuable tool for characterizing a number of multiphase processes/reactor systems of industrial interest, which use a range of particles with varying properties. For example, gas-solid fluidized beds are widely used in process industries for large-scale applications like coal gasification to small-scale polymer and pharmaceutical production. These reactors contain a large number of solids with a wide range of sizes and sometimes different densities; characterization of the flow of these solids of different physical properties can provide valuable information for designing and understanding these systems. Similarly, M-RPT can be very useful in the evaluation of multiphase processes in gas-liquid-solid (GLS) and liquid-solid (LS) fluidized beds, stirred tanks, slurry bubble columns, spouted beds, etc. To accomplish the above objectives, a new data acquisition system for tracking multiple radioactive particles was designed and manufactured. The system was developed with the help of the Oak Ridge National Laboratory (ORNL) team consisting of electronic engineers, software engineers and nuclear engineers. The hardware was assembled at the Chemical Reaction Engineering Laboratory (CREL), Washington University in St. Louis. The necessary modifications to hardware and software were made. The M-RPT electronics is capable of tracking 8 radioactive tracers simultaneously. As a proof-of-concept, the presented work explains the principle, validation and implementation of the M-RPT for tracking two tracers simultaneously; however, the procedure and algorithms for dual-particle tracking can be easily extended to track more particles. Various issues related to the design and selection of the M-RPT system and its components are discussed here. Further details about the hardware and software can be found elsewhere [49]. The procedure and the guidelines to operate the M-RPT unit are also detailed by Ref. [49].

2. Experimental setup

2.1. M-RPT hardware

Fig. 1 below shows the schematic of the new M-RPT electronics. The connections of the electronics components are shown in Fig. 2. The M-RPT unit consists of detectors formed by a photomultiplier tube (PMT) connected to the base amplifier. This base amplifier is powered by a power supply unit. The output signal from the base amplifier is fed to a

Table 1
List of possible radioactive candidates to be used for M-RPT.

Element (mass number)	Half life	Gamma energy MeV (%)	Density (g/cm^3)	Comments
Beryllium (7)	53d	0.48(10)	1.8	Poisonous
Sodium (22)	2.58y	0.511 (180),1.27 (100)	0.97	Reactive with water
Scandium (46)	84d	0.89(100), 1.12 (100)	2.9	Can be used
Manganese (54)	303d	0.83(100)	7.3	Can be used
Cobalt (56)	77.3d	0.85(100)-3.3 (13)	8.7	Many gamma energies, not suitable
Cobalt (57)	267d	0.12(87), 0.14(11)	8.7	Very low gamma energies
Cobalt (58)	71d	0.81(99), 1.7 (0.6)	8.7	Can be used
Cobalt (60)	5.26y	1.17 (100),1.33 (100)	8.7	suitable
Zinc (65)	245d	1.12(49)	7.1	Low gamma percentage
Selenium (75)	120d	0.14(57), 0.27(60)	4.8	low gamma energies
Rubidium (83)	83d	0.53(93), 0.79(1)	1.5	Spontaneously flammable in air,
Rubidium (84)	33d	0.9(74), 0.5 (42)	1.5	explosive in water
Strontium (85)	64d	0.51(100)	2.6	Reactive with water
Yttrium (88)	108d	0.9(91), 1.84 (100)	4.5	Suitable
Zirconium (95)	65d	0.72(49),0.76 (49)	6.4	Can be used
Niobium (95)	35d	0.77(100)	8.6	Can be used
Ruthenium (103)	40d	0.5(88), 0.61 (6)	12.2	Very high density
Antimony (124)	60d	0.6(97), 1.7 (50),8 to 2.1	6.68	Many gamma energies
Cesium (134)	2.1y	0.6(98), 0.8 (98)	1.87	Explosive in water, reacts with air
Cerium (139)	140d	0.165(80)	6.9	Very low gamma energy
Hafnium (175)	70d	0.34(85)	11.4	Low gamma energy, high density
Osmium (185)	94d	0.65(80), 0.88(14)	22.48	Heaviest element, oxide is poisonous
Iridium (192)	74d	0.32(80), 0.47(49)	22.4	Extremely high density

timing filter amplifier (TFA) input for amplification. Both the power supply unit and the timing amplifier sit in a NIM bin. Each timing amplifier has 8 channels (one for each detector). The timing amplifier is connected to the pulse processor card, which functions as a discriminator, scaler and an interface to the computer. This pulse processor card sits in a compact PCI (peripheral component interconnect) box and is connected to the back plane of compact PCI which also holds a PC on a card.

A single C++ program compiled and run by the user performs data acquisition according to the user's needs. Each component of the M-RPT unit, its operation and functions are explained elsewhere [49].

2.2. Selection of radioactive sources

A number of characteristics should be taken into account for the selection of radioactive sources used in the M-RPT. Some of the main considerations are as follows.

1. Gamma energy peak: The M-RPT works on the principle of discrimination between different sources based on the gamma energy peak (explained in detail in the next section). Therefore, it is necessary that at least one peak of at least one of the multiple particles should be completely separated from all other peaks of other particles. In addition, for M-RPT to work, no more than two gamma peaks of two different particles should be overlapped. This criterion narrows the radioactive sources to possible candidates for M-RPT.
2. Half-life period: To ensure that the activity of tracer particles does not change significantly during an experiment, only sources with a half-life of over a month are suitable. A relatively long half-life allows a particle to be used multiple times, however a very long half-life entails a higher level of liability on the part of the user for protecting, handling, and maintaining it.
3. Physical state: The radioactive source to be used as a tracer must be easy to handle and mimic the phase to be tracked. It cannot be compatible with the system. Radioactive sources must exist in the solid phase under normal operating conditions.
4. Density: The radioactive tracer density should match the phase being tracked. For this reason, the density of the source is manipulated in different ways to make it either lighter or heavier. This is to match the density of the phase to be tracked. A radioactive source (in solid state) can be coated with suitable material or it can be enclosed in a tiny plastic ball to adjust its density. But if the radioactive source density is very high, it would be difficult to adjust its density to the required value. Density is certainly a factor of importance in the selection of a radioactive source. However, it depends on the requirements of the system to be studied.
5. Personnel safety: The safety of personnel handling and using radioactive material is paramount. Excessive radiation exposure causes serious health problems. Thus, the selected radioactive source should possess minimum health risks. It should be easy to handle and clean up in case of contamination. The ALARA (i.e. as low as reasonably achievable) principle should be applied when dealing with the radiotracer particle. This minimizes the risk of radiation exposure to personnel, as well as the risk of contamination to the environment or other individuals. By following the ALARA principle, the radiation risks can be minimized by selecting the lowest possible activity of radioisotope that will still provide the desired results. This ensures that personnel safety is maintained while still providing accurate results.

There are many other considerations in the selection of a radioactive source such as physical and chemical properties of the source, cost, ease of availability, ease of activation and legal formalities. The radioactive source should be approved by the local Radiation Safety Department before being used.

Table 1 gives a condensed list of radioactive sources that may or may not be suitable for the M-RPT, from Ref. [50]. Only elements occurring in solid form with a half-life greater than 30 days and less than 5 years are listed in Table 1. Sources that do not produce gamma or have a very low percentage of gamma production are not listed. Upon careful consideration of all the above criteria, Co-60 and Sc-46 were selected for dual-particle tracking to evaluate the developed technique. Co-60's high-energy gamma peak is completely distinguished from Sc-46's other gamma peaks, satisfying the most crucial criterion. The half-life of Sc-46 is only 84 days, which is suitable. Co-60 has a very long half-life of 5.27 years, which is not desirable from a safety perspective, but is suitable for frequent use at no additional activation cost. Co-60 and Sc-46 are both available in the solid state with densities of 8.9 and 2.98 g/cm^3, respectively. Co-60 is heavier, meaning smaller particles are required. Smaller particles require longer activation times and are more difficult to handle. Thus, Co-60 and Sc-46 may not be the ideal candidates, but they are the most viable possible alternatives that meet most of the requirements mentioned above at this time for the development and validation of the M-RPT.

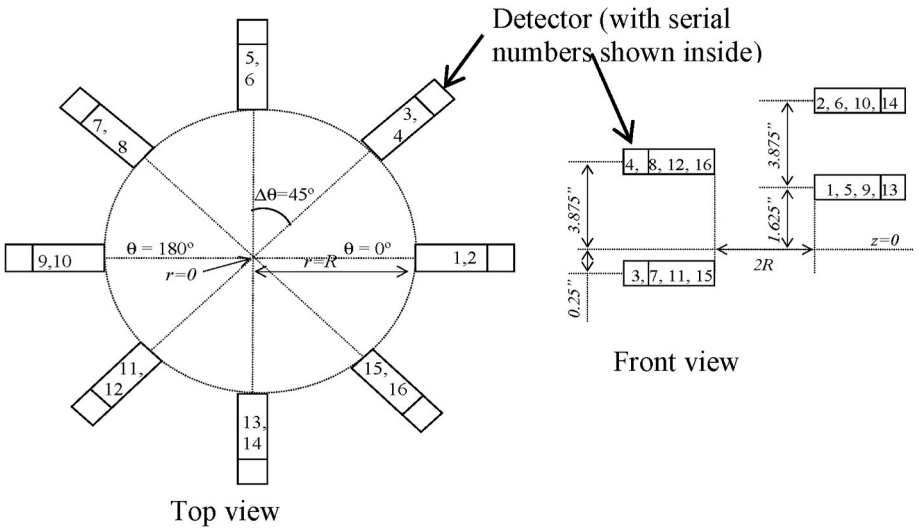

(a)

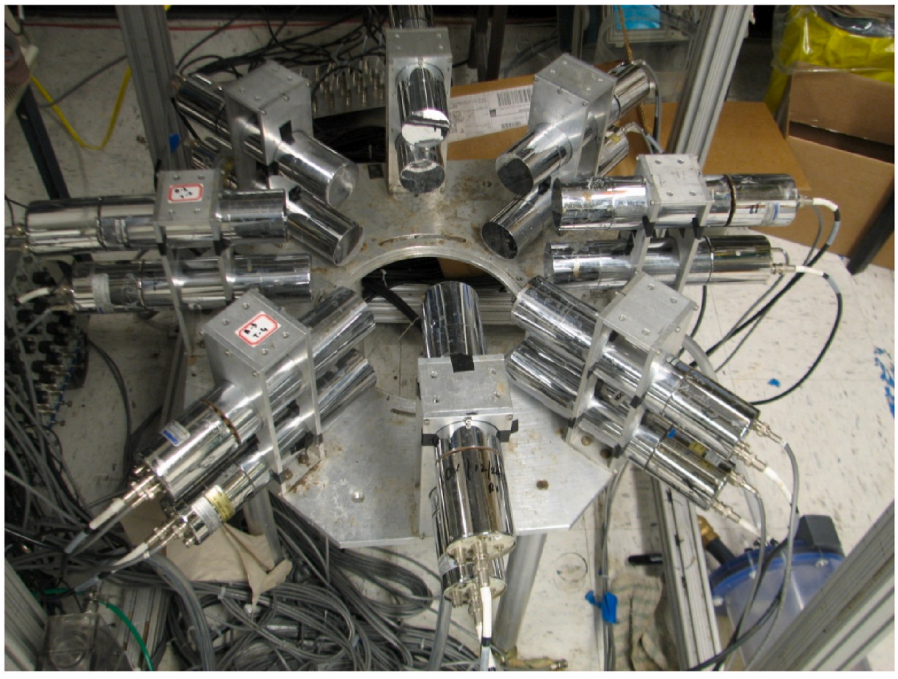

(b)

Fig. 3. (a) Schematic of the arrangement of detectors on detector stand. (b) Photograph of detector stand.

3. M-RPT validation for tracking two stationary particles

The M-RPT technique, its principles, operation, and data-processing will be discussed in this section with reference to the tracking of two stationary particles, Co-60 and Sc-46. By tracking stationary particles at known locations, the reconstruction error can be evaluated and the fault-free working M-RPT electronics can be confirmed and the reconstruction algorithm can be tested.

3.1. Experimental set-up for tracking two stationary particles

A total of sixteen sodium iodide (NaI) detectors were mounted circumferentially on a stand in eight columns separated by 45°, see Fig. 3 (a) and (b). Each column had two detectors mounted one over the other and separated by 3.9 inches (9.906 cm). A total of four detectors are used at each axial level to detect the tracer. This is more than the minimum number of detectors recommended for each level in the literature [37, 51].

An automated calibration device was used for carrying out the calibration. The device is equipped with a rod to hold the radioactive source at one end. This rod is connected to three separate motors for independent rod movement in axial, radial and azimuthal directions. The design and details of the calibration device are given in detail by Ref. [24]. Co-60 and Sc-46 were chosen as the sources due to their differing gamma-ray energies and emissions. 100 μm Co-60 particle with an approximate activity of 100 μCi was enclosed in a 1 mm polypropylene ball. The Sc-46 particle was 150 μm in diameter with an approximate activity of 150 μCi and was encapsulated in a 1 mm polypropylene ball. By enclosing the particles in plastic balls, they become convenient to handle and are more likely to be handled safely.

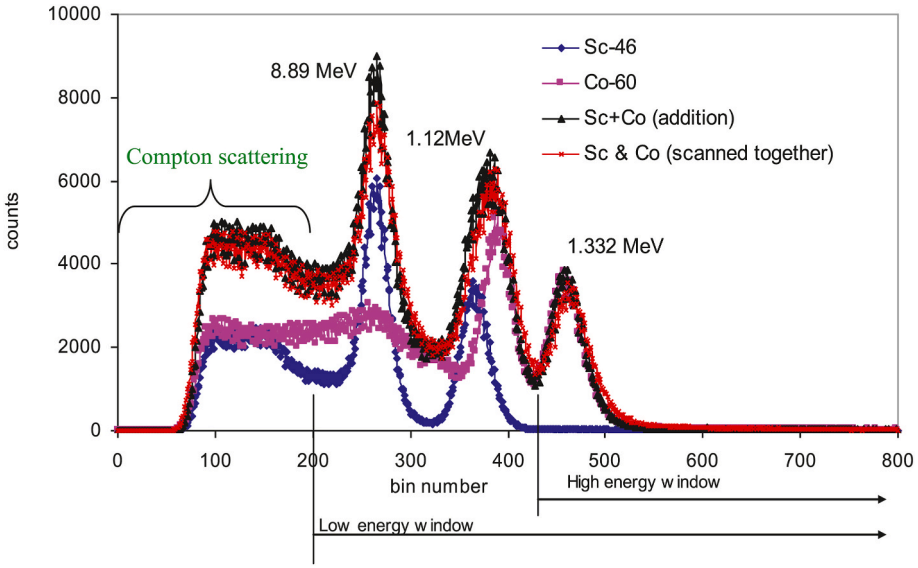

Fig. 4. Gamma peaks of Sc-46 and Co-60 individually, together and summation of individual counts.

3.2. Principle and methodology

Radioactive particle tracking technique works on the fact that the strength of the signal received by a detector from a radioactive source (number of photons) is inversely proportional to the distance between the source and the detector. Thus, by prior calibration, this proportionality can be determined and the location of a single radioactive source can be calculated. This is if photon counts are recorded. This procedure is called reconstruction of tracer locations and is described elsewhere [49]. Radioactive particle tracking technique works on the fact that the strength of the signal received by a detector from a radioactive source (number of photons) is inversely proportional to the distance between the source and the detector. Thus, by prior calibration, this proportionality can be determined and the location of a single radioactive source can be calculated. This is if photon counts are recorded. This procedure is called reconstruction of tracer locations and is described elsewhere. If more than one radioactive source is to be tracked simultaneously, it is necessary to distinguish between the photon counts emitted by each source. Following is an explanation of the principle and methodology for discriminating between counts originating from different sources.

Gamma peaks obtained by recording the photon counts emitted by Sc-46 and Co-60 in fine mode (fine mode records the counts of all energies as opposed to coarse mode, where only the counts in a selected energy window are recorded) for one detector are shown in Fig. 4. The procedure to obtain scans and operate the M-RPT unit is described by Ref. [49]. To obtain the counts for generating gamma peaks, radioactive sources can be placed anywhere within the vicinity of all the detectors. The counts obtained from radioactive particles are additive. The total counts of Sc-46 and Co-60 obtained individually are equal to the counts obtained from both sources together, as illustrated in Fig. 4. Fig. 4 reveals a very important feature that forms the principle for discriminating between different radioactive sources. The high energy peak of Co-60 (1.332 MeV) is completely separated from other peaks of Sc-46 and low energy peak of Co-60 itself. Thus, if the photon counts of Sc-46 and Co-60 are collected in such a way that the high energy counts of Co-60 are recorded separately, then reconstruction of Co-60 is a trivial problem similar to reconstruction of a single particle in CARPT. The additive property of counts can be used for Sc-46 particle reconstruction.

3.3. Selection of energy windows

The counts of high energy and low energy peaks are separated by setting up the energy windows for the discriminator. The M-RPT unit is capable of recording counts in eight separate energy windows. The lower and upper limit of each window can be specified by the user; the windows can also be overlapped if necessary. Setting 8 separate energy windows provides the possibility of tracking eight different radioactive sources simultaneously. However, tracking and reconstruction of only two radioactive sources is discussed here. This technique once validated can be extended easily to track more than two radioactive sources.

The first step in the M-RPT is to obtain the position of energy peaks of Sc-46 and Co-60 for each detector, as shown in Fig. 4. The limits of the energy window for calibration and tracking experiment are obtained from Fig. 4. The complete energy spectrum is spread from 0 to 1023 bins (each bin number corresponds to an energy value) by discriminator. Lower and higher limit of high energy window can be 425th and 600th bin, respectively. Thus, all the counts corresponding to the energy level from 425th to 600th bin (both inclusive) will be recorded in high energy window. The higher limit can be extended till 1023rd bin, this will necessarily make no difference because the counts of both the sources are zero from bin number 525 onwards. But the lower limit has to be specified higher than 425th bin, such that the counts of Co-60 can be recorded distinctly without any overlap from Sc-46. The lower and higher limit for low energy window can be 200th and 425th bin, respectively. Again, the lower limit can be as low as bin number zero. But the Compton scatter present in lower bin numbers below 200 introduces error during reconstruction and must be avoided. Thus, the lower limit is set at 315th bin to exclude Compton scattering by Sc-46 as well. The low span of energy window reduces the number of counts in the window. Lower counts also introduce error in the reconstruction. If the activity of the sources used is high, then the low span of the energy window is acceptable. Very high activity of sources however, will cause the problem of peak shift [49].

A careful consideration should be given to select the limits of energy windows as explained above. Every detector can have different specifications of limits of energy windows based on the detector settings.

3.4. Calibration

Two sets of calibration are required for (stationary or moving) dual particle tracking; one for each source, Sc-46 and Co-60, separately. Same

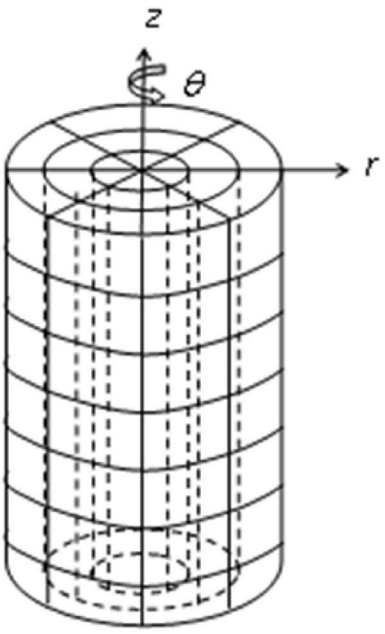

Fig. 5. Grids for calibration points/locations.

Table 2
Cylindrical coordinates of calibration points.

r (inch)	θ (degrees)	z (inch)	Number of calibration points
0	0	0 to 4.5 (with Δz of 0.5)	1 × 1 × 10 = 10
1	0 to 330 (with Δθ of 30)	0 to 4.5 (with Δz of 0.5)	1x12x10 = 120
2	0 to 330 (with Δθ of 30)	0 to 4.5 (with Δz of 0.5)	1x12x10 = 120
Total number of calibration points			250

limits of energy windows and data acquisition frequency should be used for both calibration and tracking. The data acquisition frequency of 50 Hz (50 samples per second) is selected in this case. Data acquisition frequency cannot be too high or too low for tracking moving particles. Very high values, normally above 200 Hz, introduce noise into the acquired data. The lower limit of allowable acquisition frequency depends on the maximum velocity of moving particles in the system. Low frequencies can cause error in reconstruction, referred to as dynamic bias [23,37].

For calibration, each particle is placed individually (in the absence of the other source) at several known locations and photon counts are recorded in coarse mode. 512 samples of photon counts are recorded at each location; each sample contains counts emitted for 0.02 s corresponding to 50 Hz frequency. The average of all the samples for each calibration location is used for reconstruction. Thus, maximum possible number of samples should be obtained during calibration for better accuracy.

The number of calibration points depends on the geometry of the system. Maximum possible number of calibration points should be used. Generally, the geometry of a system is divided into number of cells in radial, azimuthal and axial direction as shown in Fig. 5, the calibration points can be located either at the centers of the cells or at the nodes of the cells for convenience. The closer the calibration points are placer, more the number of calibration points, thus lesser is the error in reconstruction of particle positions. 250 calibration points were used for tracking stationary particle, in this case. The cylindrical coordinates of calibration points are listed in Table 2. The fully automated calibration process integrated within the data acquisition program records both the calibration locations (r, θ and z) and the counts.

The calibration locations for both the particles should preferably (not necessarily) be the same. If counts of Sc-46 and Co-60 together at 'position x' are required, they can be evaluated by summing up the individual counts of Sc-46 and Co-60, each recorded at the same 'position x'.

The calibration data is obtained in two separate energy windows as explained earlier. Fig. 6(a) and (b) show the calibration plot for Sc-46 and Co-60, respectively, for both energy windows for a particular detector. The coordinate in Fig. 6(a) and (b) is the averaged value of counts obtained for 512 samples. The abscissa is the distance of the source from the given detector. The number of counts varies inversely with the distance from the detector; the counts recorded are higher when the source is nearer to the detector and vice-versa. In Fig. 6(b), for Sc-46, the counts in the high energy window are very low; they should be ideally zero, as the Sc-46 peaks do not fall in the high energy. Non-zero counts are recorded due to the background radiation and/or the random nature of radioactivity which introduces error in the reconstruction.

3.5. Stationary tracking experiment

During the actual tracking experiment, Co-60 and Sc-46 particles were placed together at 48 known locations and counts data was obtained according to specified energy windows during calibration. 64 samples of data at frequency of 50 Hz were obtained for each of 48

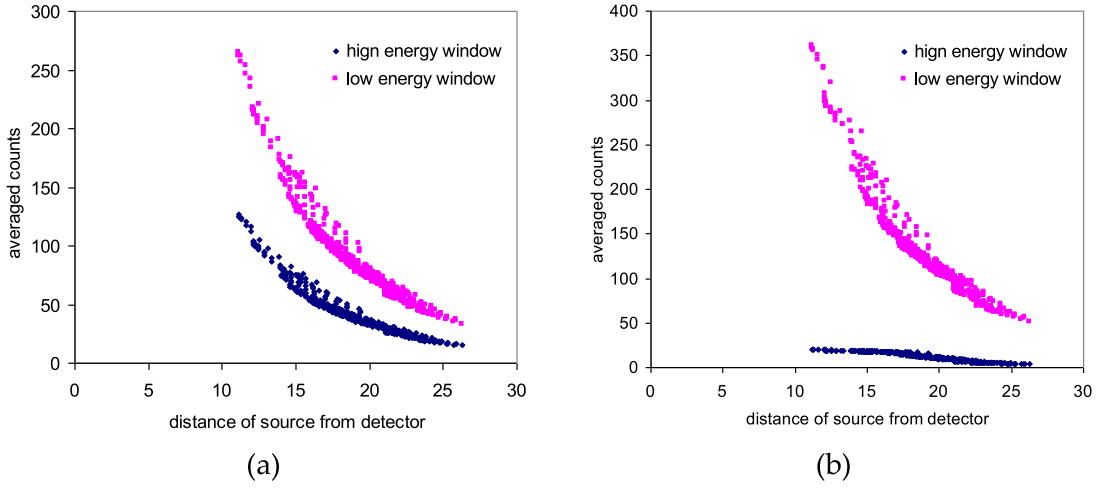

Fig. 6. (a) Calibration plot for Co-60 and (b) calibration plot for Sc-46.

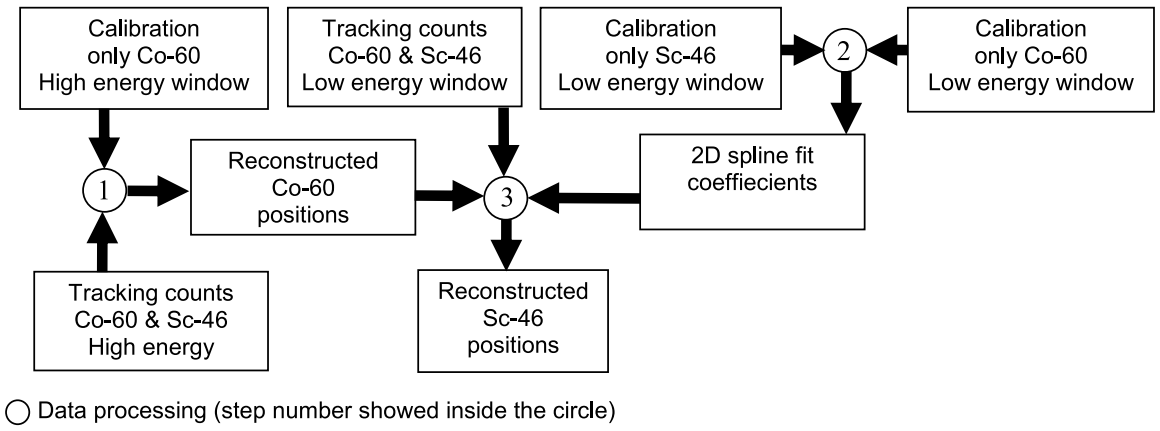

Fig. 7. Modified reconstruction algorithm for dual-particle tracking.

known locations. 24 of these locations were same as calibration points. Reconstruction of tracer locations different from calibration locations enables critical testing of the accuracy of the reconstruction algorithm. The particles were placed at r = 1 inch, θ = 0°–345° with Δθ = 15°, and z = 2 and 3 inches, thus totaling 1x24x2 = 48 locations.

Traditionally for tracking a moving particle in any reactor system, the particle is released into the system and it is tracked for at least a period of 24 h at a suitable data acquisition frequency so that the tracer has a chance to visit multiple times to every portion of the system and statistically meaningful data is obtained. Since the particles were kept at known stationary locations longer acquisition times were not required.

3.6. Reconstruction results

Obtaining the location of the radioactive particles from the acquired count data is called particle position reconstruction. The reconstruction algorithm is shown in Fig. 7. Since the limits of high energy window are selected such that only counts of Co-60 are recorded in that window, the reconstruction procedure of Co-60 is exactly similar to that of single particle CARPT. Reconstruction algorithm applied for reconstructing the tracer positions is the weighted least-squares method [14,22,37]. The weighted least-squares method is a widely used technique in various fields, including image processing, computer vision, and medical imaging. This algorithm is known for its ability to accurately reconstruct and estimate unknown parameters by minimizing the sum of the weighted squared differences between the observed and estimated values. In the context of tracer position reconstruction, the weighted least-squares method proves to be an effective approach for obtaining accurate and reliable results. Reconstruction procedure of single particle tracking is explained in short here, see Ref. [49] for more details.

The first step is to reconstruct the Co-60 positions. The calibration curve of Co-60 (for high energy window) is fitted using spline fitting and spline coefficients are obtained for each detector [18]. These spline coefficients can then be used to calculate the position of Co-60 for each detector, which can then be used to reconstruct the trajectory of the Co-60 particle. Using these coefficients and the known counts of Co-60 in the high energy window for a particular detector, the distance of particle from that detector can be evaluated. The spline fitting technique provides an efficient way to fit a curve to the data points, which can then be used to calculate the position of the Co-60 particle accurately. By using the known counts of Co-60 in high energy windows, the distance of the particle can be determined with a high degree of accuracy. This can then be used to accurately reconstruct the trajectory of the Co-60 particle. For every tracked location of the Co-60 tracer, there are three unknown coordinates (x, y and z) and N number (equal to number of detectors) of calculated distances of Co-60 from each detector (see equation (1)).

$$d_i = \sqrt{(x - x_i)^2 + (y - y_i)^2 + (z - z_i)^2} \quad for\ \ i = 1\ \ to\ \ N \tag{1}$$

where, d_i is the distance of tracer from i^{th} detector

(x_i, y_i, z_i) are the coordinates of ith detector

N is the number of detectors (>3).

Thus, a system of N nonlinear equations can be solved using a least square approximation method to evaluate three unknowns. The least square approximation function is given in equation (2). The least squares approximation method works by minimizing the sum of the square of the residuals, which is the difference between the known values and the measured values.

$$f(x, y, z) = \sum_{i=1}^{N} \left\{ \left[(x - x_i)^2 + (y - y_i)^2 + (z - z_i)^2 \right] - d_i^2 \right\} \tag{2}$$

The reconstructed positions evaluated in this manner are then filtered to remove any noise in the processed data, encountered due to the random nature of radioactivity. An alternative is the cross-correlation method formulated by Ref. [52] which can be more accurate but a computationally time-intensive method of reconstruction. The next step in reconstructing the Sc-46 locations is explained in the following section.

In the first step, 2D (two-dimensional) spline fitting is done using three variables, the total counts of Co-60 and Sc-46, distance of Co-60, and distance of Sc-46 from a particular detector. By knowing two of these variables, the third unknown can be evaluated by the spline coefficients obtained through 2D spline fitting. Distance of Co-60 from any detector is known, because Co-60 positions are reconstructed. Total counts of Co-60 and Sc-46 are available in the low energy window from tracking experiment. Thus, the third unknown distance of Sc-46 from every detector can be evaluated using 2D spline fit coefficients.

The second task would be to generate a 2D spline fit plane. Calibration counts of only Co-60 and only Sc-46 from low energy window can be added to obtain total counts of Co-60 and Sc-46 in low energy window, as shown below. By combining the individual detector counts with the 2D spline fit coefficients, a 2D spline fit plane can be generated which can accurately determine the unknown distance of Sc-46 from each detector.

Calibration counts of Co-60 for i^{th} detector, $C_i = \left[c_1 \quad c_2 \quad c_3 \ldots \ldots c_j \ldots \quad c_n \right]_i$.

Calibration counts of Sc-46 for i^{th} detector, $S_i = \left[s_1 \quad s_2 \quad s_3 \ldots \ldots s_j \ldots \quad s_n \right]_i$.

Total counts of Co-60 and Sc-46 for i^{th} detector,

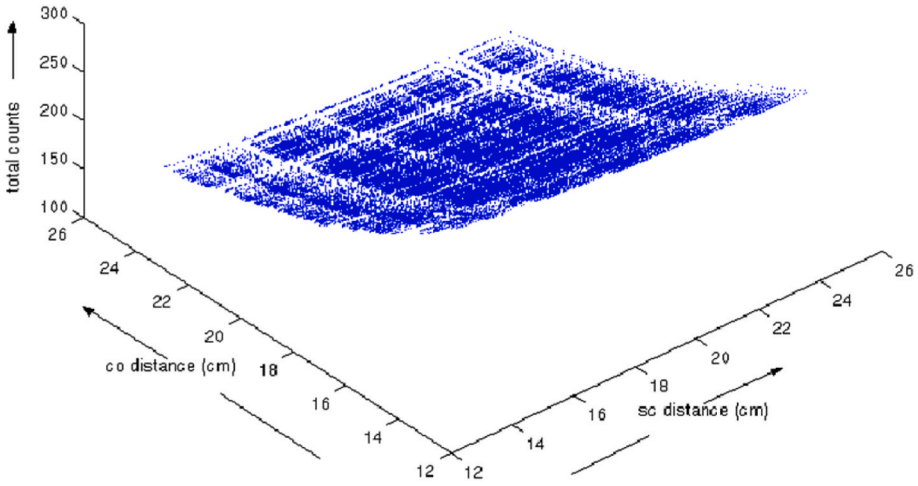

Fig. 8. Calibration plane for a detector.

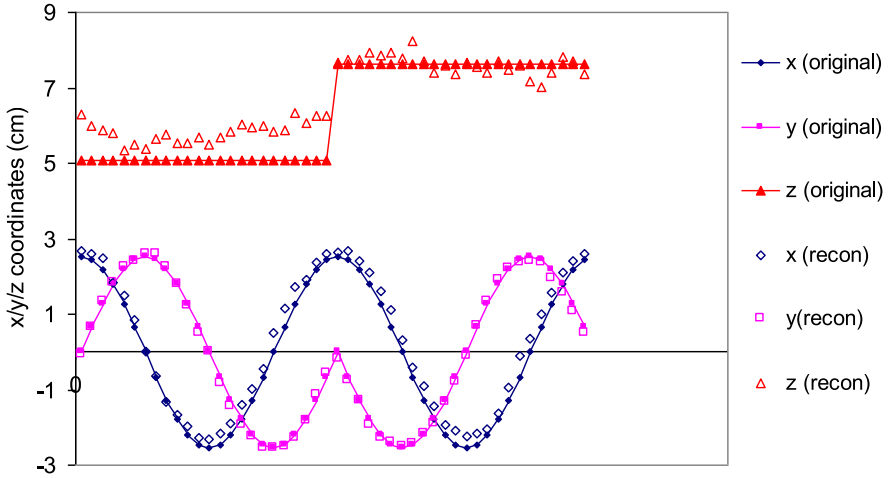

Fig. 9. Comparison of reconstructed Co-60 locations with experimental positions.

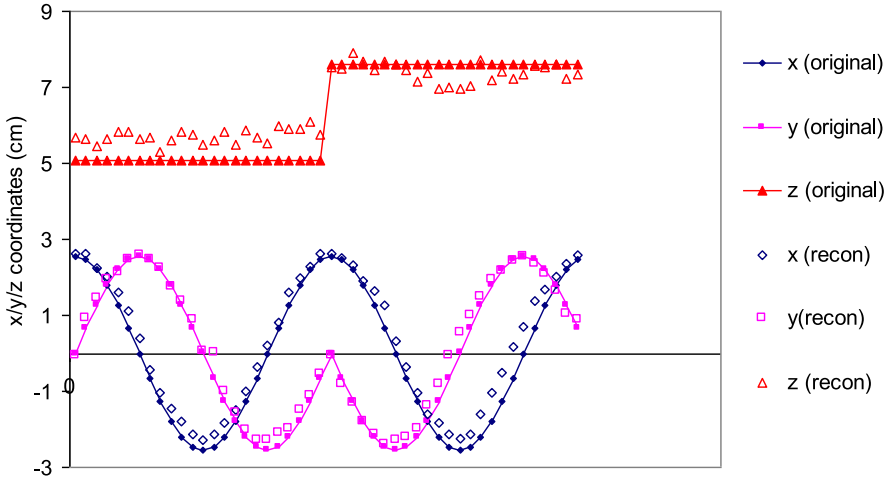

Fig. 10. Comparison of reconstructed Sc-46 locations with experimental positions.

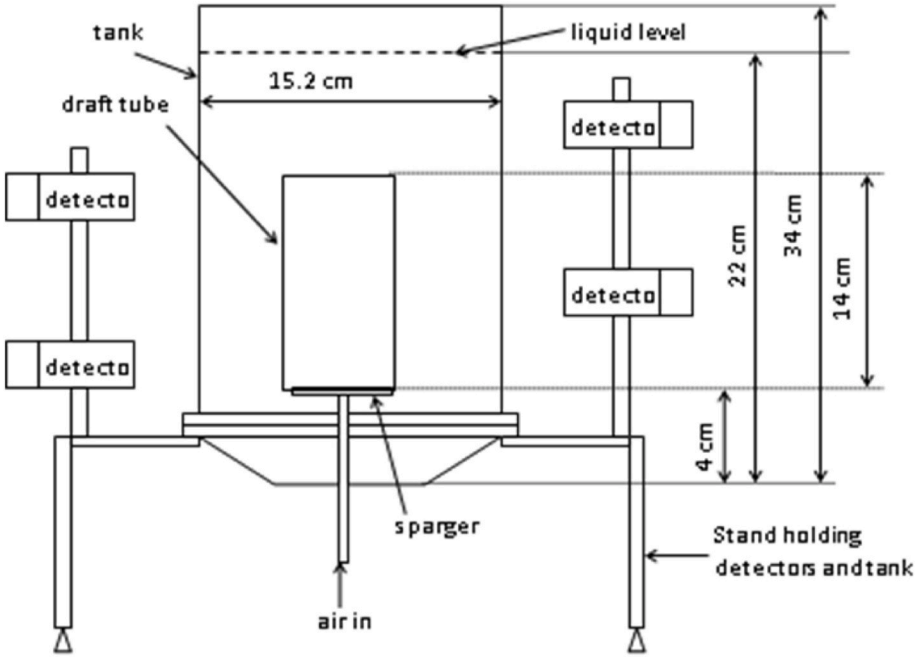

Fig. 11. Experimental set-up for dual particle tracking.

$$T_i = \begin{bmatrix} t_{1,1} & t_{1,2} & \ldots t_{1,k} \ldots & \ldots & t_{1,n} \\ t_{2,1} & t_{2,2} & \ldots & \ldots & \ldots \\ \ldots t_{j,1} \ldots & \ldots & t_{j,k} & \ldots & t_{j,n} \\ \ldots & \ldots & \ldots & \ldots & \ldots \\ t_{n,1} & t_{n,2} & \ldots & \ldots & t_{n,n} \end{bmatrix}_i \quad where, t_{j,k} = c_j + s_k$$

Where c_j are the counts of Co-60 at the calibration location j.

s_k are the counts of Sc-46 at the calibration location k

$t_{j,k}$ are the total counts of Co-60 and Sc-46 with Co-60 at the calibration location j and Sc-46 at the calibration location k

n is the total number of calibration points.

Every count c_j in matrix C_i is associated with distance $d^{c}_{j,i,}$ i.e. distance of Co-60 at j^{th} location from i^{th} detector. Similarly, every count s_j in matrix S_i is associated with distance $d^{s}_{j,i,}$ i.e. distance of Sc-46 at j^{th} location from i^{th} detector, such that;

Distance of Co-60 and Sc-46 calibration locations from i^{th} detector, respectively, are

$$D^c_i = \begin{bmatrix} d^c_{1,i} & d^c_{2,i} & \ldots d^c_{j,i} \ldots & d^c_{n,i} \end{bmatrix}$$

$$D^s_i = \begin{bmatrix} d^s_{1,i} & d^s_{2,i} & \ldots d^s_{j,i} \ldots & d^s_{n,i} \end{bmatrix}$$

Using matrix D^c_i, D^s_i and T_i, 2D spline fit plane can be generated and spline fit coefficients can be obtained. Unlike a calibration curve in 1D spline fitting, a calibration plane is generated, as shown in Fig. 8. The 2D spline fit plane can be used to represent the relationship between the distance of Sc-46 from each detector and the count rate of each detector. This allows the unknown distance of Sc-46 from each detector to be determined from the count rate of each detector. Furthermore, the combination of the individual detector counts and the 2D spline fit coefficients enables a more precise determination of the unknown distance of Sc-46 from each detector (see Fig. 8).

In the third step, using the total counts of Co-60 and Sc-46 in low energy window from tracking experiment and corresponding reconstructed distance of Co-60 for each count data, distance of Sc-46 from each detector can be evaluated. Again, as described above, by least square approximation of these distances, coordinates of Sc-46 can be evaluated and filtered to reduce the error introduced due to the random nature of radioactivity.

The reconstruction of Co-60 and Sc-46 locations using the above algorithm is shown in Figs. 9 and 10, respectively. The error in reconstruction of Co-60 is less than 5% for x and y coordinates whereas 15% for z coordinates because the calibration grid in z direction was coarser than in x and y direction. The error in reconstruction of Co-60 is less than Sc-46 because the Sc-46 counts do not interfere with Co-60 in the high energy window. But the error in reconstruction of Sc-46 is higher than for Co-60 because the error in Co-60 reconstruction is further propagated and amplified in Sc-46 reconstruction. The reconstruction results of Co-60 and Sc-46 scanned together with the new M-RPT unit show that the M-RPT unit can be satisfactorily used to track two particles simultaneously. Thus, the new technique M-RPT is validated for tracking two stationary radioactive sources successfully. In the next section the same methodology will be implemented to track Co-60 and Sc-46 together while moving independently in a cold reactor system.

4. M-RPT validation for tracking two moving particles

Both old single particle CARPT and M-RPT units were used for this validation experiment. The objective was to evaluate the results of the new unit with the benchmarked data obtained by the old CARPT unit and ensure that the M-RPT unit is providing correct results for tracking two moving particles.

4.1. Experimental set-up for tracking two moving particles

An acrylic tank of 15.2 cm diameter and 34 cm in height, as shown in Fig. 11, was used in this experiment. Tank was equipped with a sparger to circulate air and a draft tube with 7.6 cm diameter and 14 cm height. Tank was filled with water up to a level of 22 inches. Air was sparged at a rate of 5 lpm. The tank was placed on a detector stand (shown in Fig. 3 (a) and (b)) in the center surrounded by 16 NaI detectors arranged circumferentially.

Co-60 and Sc-46 were used as the radioactive sources. 100 μm Co-60 particle with approximate activity of 100 μCi and 150 μm Sc-46 particle with approximate activity of 150 μCi was used. Both particles were enclosed in 1 mm polypropylene balls and the density was adjusted equal to that of water to mimic the water phase.

Five sets of experiments were performed; tracking Co-60 and Sc-46 individually with both the old single particle CARPT unit and the new

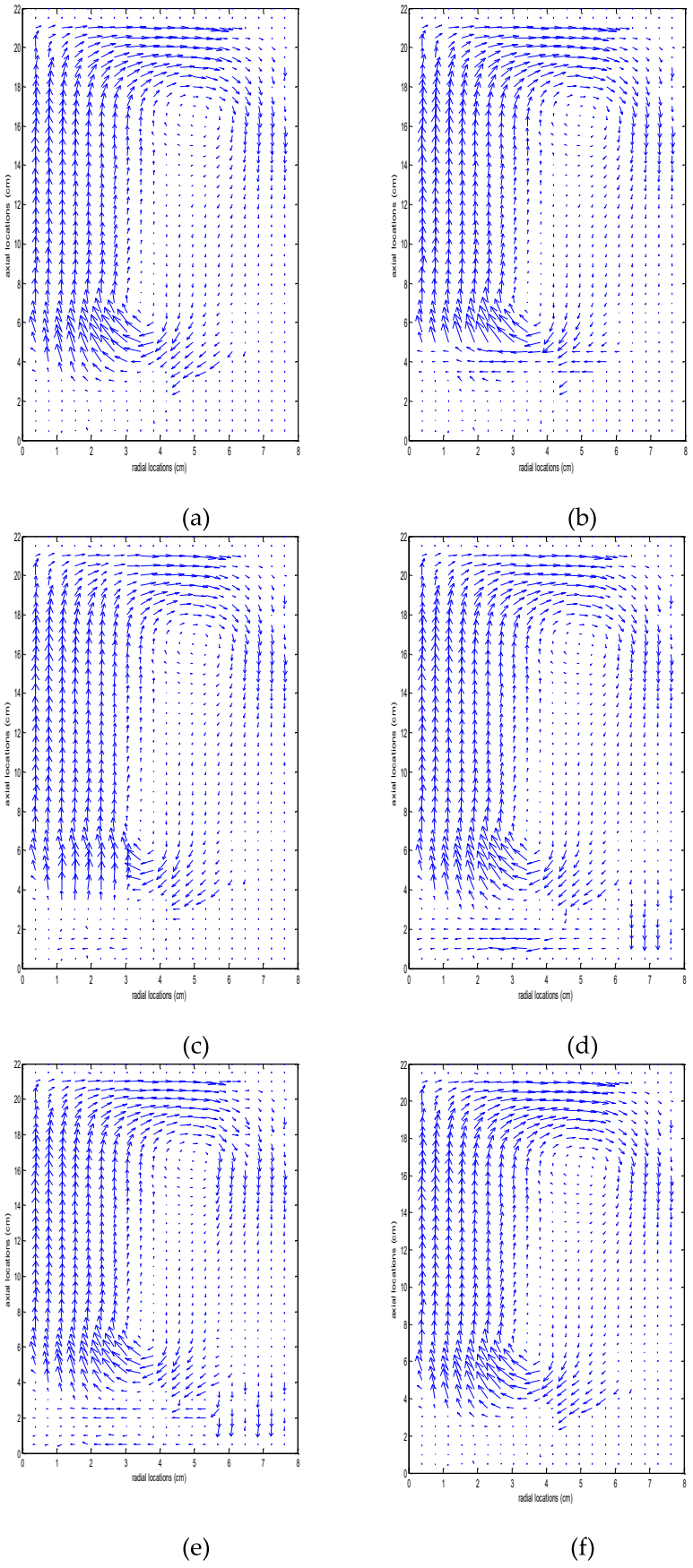

Fig. 12. (a) and (b) Flow pattern obtained from single particle CARPT unit. (c) and (d) Flow pattern obtained from M-RPT unit for single particle. (e) and (F) Flow pattern obtained from M-RPT unit for dual tracking. y-axis is the axial locations in (cm), and x-axis is radial locations in (cm).

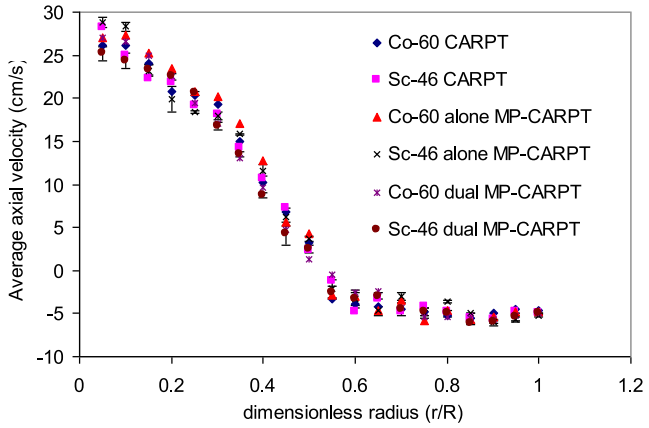

Fig. 13. Comparison of average axial velocity profiles at the center of the tank.

M-RPT and tracking Co-60 and Sc-46 together with M-RPT. For M-RPT unit, the limits of low energy window were set from bin number 200 to 425, whereas the limits of high energy window were set from bin number 425 to 600. Calibration was carried out separately for the old and the new unit at 500 different known locations for individual Co-60 and Sc-46 particles using both units. The data acquisition frequency was 50 Hz. For the tracking experiment radioactive particles were introduced into the system and data was acquired for a period of 24 h at a frequency of 50 Hz for each experiment.

4.2. Reconstruction results

The M-RPT algorithm (Fig. 7) was used for reconstruction of Sc-46 positions from the dual particle tracking data. For all other tracking experiments, the reconstruction was treated as in single particle tracking. The reconstructed position data is actually instantaneous position data for the particle. Since the acquisition frequency is known (50 Hz), the time lap between 2 consecutive positions is also known (0.02 s). The instantaneous position data can be processed to obtain instantaneous velocities. Time averaged, azimuthally averaged axial and radial velocities can be obtained from instantaneous velocity data and this can be used to obtain time averaged flow pattern of moving particles along with turbulence quantities. Post-processing of reconstructed data is explained in detail in Ref. [49].

The flow patterns obtained from each of the tracking experiments. For Co-60 and Sc-46 with the old CARPT unit, Co-60 and Sc-46 tracked separately with the M-RPT unit and Co-60 and Sc-46 tracked together with the new M-RPT unit are shown in Fig. 12(a) to 12(f), respectively. The flow patterns look more or less the same and the differences between the data are not obvious.

Radial profiles of time averaged azimuthally averaged axial velocities at the center of the tank are compared in Fig. 13 to evaluate the quantitative differences between the data obtained from old unit and new unit, and between the single particle tracking and dual particle tracking. The magnitude of axial velocity is slightly different for every case. If the velocities at a given location obtained from single particle tracking of Co-60 and Sc-46 are averaged and used as a basis to evaluate the error, then the reconstruction error is less than 10%. This (±10%) error is acceptable and is within the range associated with CARPT itself [18,52].

It can also be noted in Fig. 13 that the error is higher at the center and negligible near the wall. Because higher counts are obtained when the particle is closer to the detectors (near the wall) as compared to when the particle is away from the detectors (at the center).

5. M-RPT validation for tracking two moving particles of different densities

Majority of the processes of industrial interest are multiphase in nature and consist of solid particles suspended in liquid or gas phase. In such processes it is of particular interest to evaluate the effect of the presence of one phase on the hydrodynamics of the other phase. This can be done using the single particle CARPT by repeating the tracking for each phase separately as only one phase can be tracked at a time. Using the M-RPT both phases can be tracked together at the same time, thus the time required for such experiments is considerably reduced. However, there are certain limitations to performing such experiments, especially to track liquid phase in a LS or GLS system. These limitations will be discussed in the following sections. To demonstrate the use of M-RPT to track two tracers representing different phases a low H/T slurry bubble column reactor (SBCR) (i.e., the term "low H/T" refers to the low height-to-diameter ratio of the reactor) with low solids loadings was used. SBCR consists of solids moving in a liquid phase agitated by gas sparging.

5.1. Experimental set-up for tracking two moving particles of different densities

The same set-up as shown in Fig. 11 was used in the experiment, but the draft tube and sparger were replaced with a distributor plate located over the conical bottom section of the tank. The plate had 139 holes of 1.32 mm diameter each, arranged in a triangular pitch of 1 cm and an open area of 1.04%. The system was operated as a slurry bubble column reactor (SBCR). The tank was filled with 4 L of water. 40 gms of 300 μm glass spheres (2.5 gm/cc density) were added to the water, such that the slurry had 1% (by weight) solids. Air was sparged at the rate of 50 SCFH, such that the superficial gas velocity in the tank was 2.154 cm/s. The average gassed liquid height was 22 cm.

A 300 μm Sc-46 particle with an approximate activity of 100 μCi was used to mimic the solid phase. The Sc-46 particle was actually 276 μm in diameter which was coated with polypropylene layer up to 300 μm to adjust its density to 2500 kg/m^3. The Co-60 particle was 100 μm in diameter and 100 μCi in strength. Co-60 particle was enclosed in a 1 mm polypropylene ball and its density was adjusted to 1000 kg/m^3 using glue to fill the air gap. The Co-60 particle was used to the liquid phase (water).

The same 16-detector set-up (shown in Fig. 3(a) and (b)) was used in this study. Three sets of experiments were performed, all of them using M-RPT unit. Two experiments were conducted where Co-60 and Sc-46 particles were tracked separately as liquid phase and solids phase, respectively. For the third set, both the particles were released in the system and were tracked together. This allowed the validation of results of dual-particle tracking of different densities against the single-particle tracking results. At a data acquisition frequency of 50 Hz, 527 calibration points were obtained for each particle and 512 samples were collected for each calibration point. The limits of the low energy window were set from bin number 250 to 475, whereas the limits of the high energy window were set from bin number 475 to 640. In each of the three experiments particles were tracked for a total of 20 h at a frequency of 50 Hz.

5.2. Reconstruction results

Single-particle tracking reconstruction algorithms were used for single-particle tracking and for Co-60 reconstruction in dual-particle tracking, whereas the M-RPT algorithm was used for reconstruction of Sc-46 in dual-particle tracking. The flow patterns obtained for Sc-46 and Co-60 are shown in Fig. 14(a) to d. The flow patterns for Co-60 from single-particle and dual-particle tracking are similar. This is also the case for Sc-46 particles. It is very interesting to note that the flow patterns at a low L/D SBCR are significantly different from the flow patterns of solids

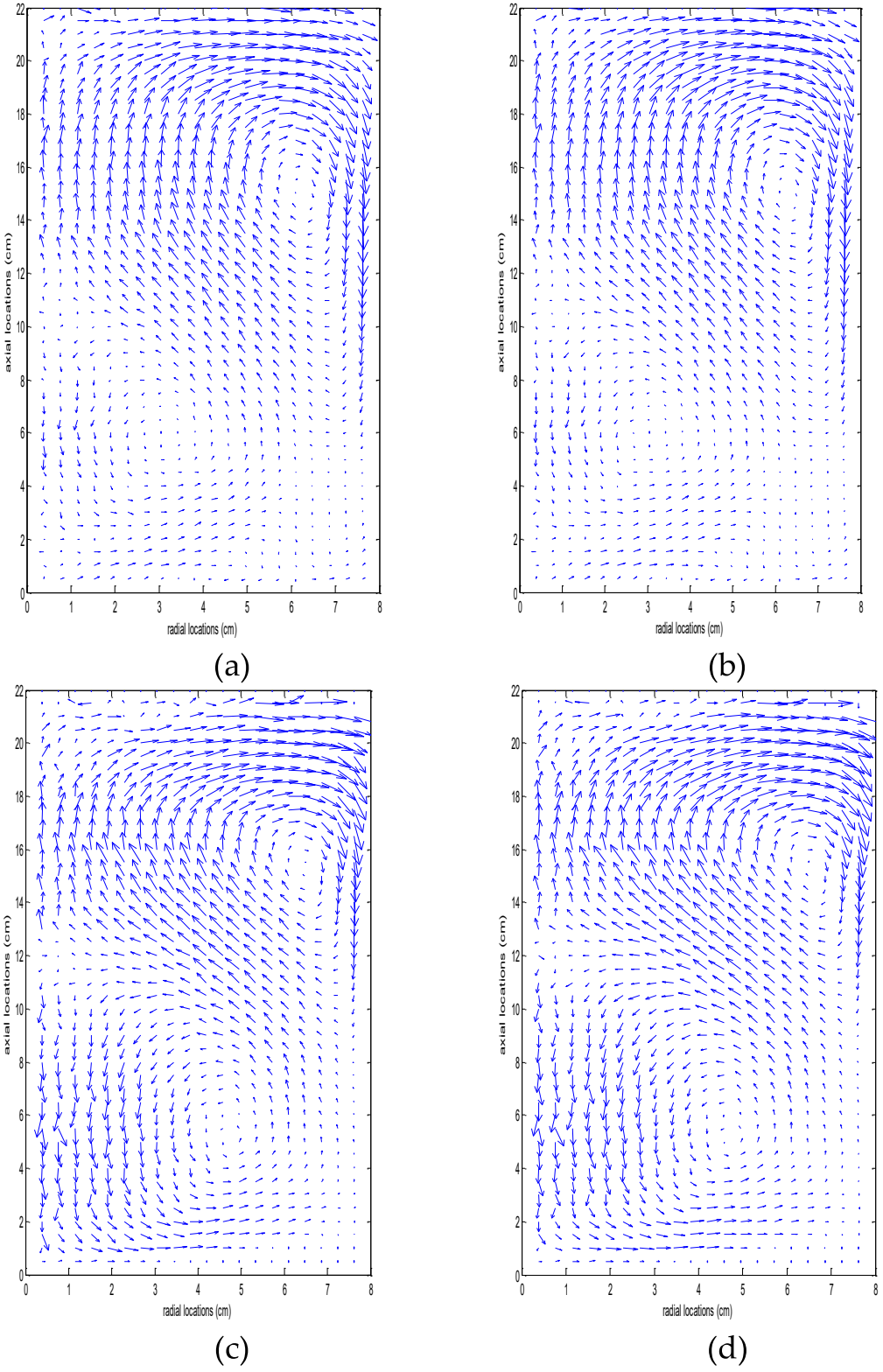

Fig. 14. Co-60 liquid phase (a) single-particle tracking (b) dual-particle tracking
Sc-46, solid phase (c) single-particle tracking (d) dual-particle tracking. y-axis is the axial locations in (cm), and x-axis is radial locations in (cm).

or liquid phases at a high L/D SBCR [18]. Fig. 15 shows the radial profile of azimuthally averaged axial velocity at the center of the column. The dual particle tracking experiment was repeated twice to obtain the error bars shown in Fig. 15. It can be seen that the difference between velocities obtained from the single-particle and dual-particle tracking is not significant (less than 5%). The error associated with CARPT itself is ±10% [38,52]. The error associated with Sc-46 reconstruction is more than the error associated with Co-60.

These results show the new M-RPT unit's ability to track two radioactive particles of different densities. However, the solids fraction in the system was kept low to 1%, such that the collisions between the

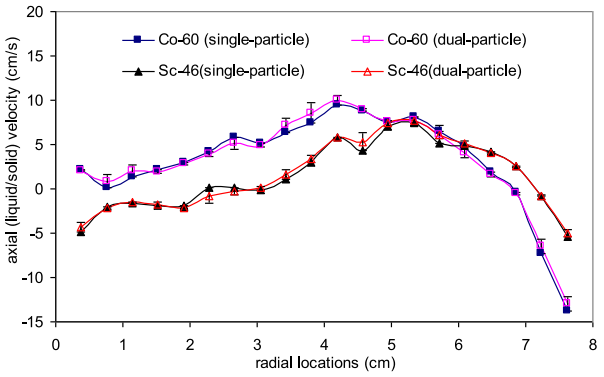

Fig. 15. Comparison of axial velocity profiles obtained from single-particle and dual-particle tracking for Co-60 and Sc-46 representing liquid and solid phase, respectively.

Co-60 particle (tracking liquid phase) and the solids in the system can be kept to a minimum. Because of the interference created by solids in the system to the tracer mimicking liquid phase, the true hydrodynamics of liquid phase cannot be determined in a high solids hold up system.

6. Remarks

- New M-RPT unit offers a number of advantages over the old single particle CARPT unit. The new M-RPT unit is compact, cheaper, faster, and easy to use and operate. It provides ability to track eight different radioactive sources simultaneously. The selection criteria for radioactive sources however limit the use of M-RPT to its full capability. Thus, the technique was validated for dual particle tracking and the same can be extended to track more than two particles simultaneously.
- The M-RPT electronics and technique was methodically validated in three steps to simultaneously track, two stationary particles, two moving particles of same density and two moving particles of different densities. The reconstruction algorithm was implemented for tracking the multiple particle which showed error of less than 10% in reconstruction of both Co-60 and Sc-46 particles in all steps.
- When tracking two different phases, ex. solid and liquid, care should be taken to design the experiment in such a way that the tracer follows the represented phase as closely as possible. Collisions of tracer representing liquid phase with the solid particles in the system should be avoided or minimized by using very low solids fraction.
- M-RPT can be used conveniently to track two or more solids phases in a system with different properties (for example size, shape or density). However, how much difference in size or density of tracers is required so that the tracers can provide true hydrodynamics of the phase being tracked needs to be evaluated. This issue can be addressed by tracking tracers of the same size and different densities or same density and different sizes and observing the difference in hydrodynamics.
- The error in the reconstruction of the M-RPT can be further reduced by some modifications of the experimental set-up, procedures, and the reconstruction algorithms. If the number of detectors is increased and are packed closely together, then the error in the reconstruction will be reduced due to increased spatial resolution. The current M-RPT reconstruction algorithm is based on the principle of addition of the calibration counts of Co-60 and Sc-46 obtained separately to represent the counts obtained together. Instead, if the calibration is performed with the Co-60 and Sc-46 particles present together, keeping one particle fixed at one location and placing other particle at all the calibration locations one by one and thus covering all the possible permutations, then more accurate calibration region can be obtained. This calibration technique will take into consideration the effect of the presence of two particles together on their total counts. In addition, if the number of calibration points is increased, it will also help to increase the accuracy of reconstruction. The reconstruction method developed by Ref. [52] can be also be used for the increased accuracy.

Declaration of competing interest

The authors declare that they have no known competing financial interests or personal relationships that could have appeared to influence the work reported in this paper.

Acknowledgments

The authors would like to thank the United States Department of Energy for sponsoring the research project (Identification Number: DE-FC36-01GO11054), and the Oak Ridge National Laboratory group for their support.

References

[1] M.H. Al-Dahhan, Radioisotopes applications in industry: an overview, Atoms For Peace An Int. J. 2 (2009) 324–337, https://doi.org/10.1504/AFP.2009.027866.
[2] M.P. Dudukovic, Opaque multiphase flows: experiments and modeling, Exp. Therm. Fluid Sci. 26 (2002) 747–761, https://doi.org/10.1016/S0894-1777(02)00185-1.
[3] M.A.S. Mohd Yunos, S.A. Hussain, S.M. Sipaun, Industrial radiotracer application in flow rate measurement and flowmeter calibration using 99mTc and 198Au nanoparticles radioisotope, Appl. Radiat. Isot. 143 (2019) 24–28, https://doi.org/10.1016/j.apradiso.2018.10.008.
[4] V. Khane, I.A. Said, M.H. Al-Dahhan, Experimental investigation of pebble flow dynamics using radioactive particle tracking technique in a scaled-down Pebble Bed Modular Reactor (PBMR), Nucl. Eng. Des. 302 (2016) 1–11, https://doi.org/10.1016/j.nucengdes.2016.03.031. *Part A*.
[5] V. Khane, M.M. Taha, M.H. Al-Dahhan, Experimental investigation of the overall residence time of pebbles in a pebble bed reactor (PBR) using radioactive pebble, Prog. Nucl. Energy 93 (2016) 267–276, https://doi.org/10.1016/j.pnucene.2016.09.001.
[6] N. Ali, T. Al-Juwaya, M. Al-Dahhan, An advanced evaluation of spouted beds scale-up for coating TRISO nuclear fuel particles using Radioactive Particle Tracking (RPT), Exp. Therm. Fluid Sci. 80 (2017) 90–104, https://doi.org/10.1016/j.expthermflusci.2016.08.002.
[7] N. Ali, T. Al-Juwaya, M. Al-Dahhan, An advanced evaluation of the mechanistic scale-up methodology of gas–solid spouted beds using radioactive particle tracking, Particuology 34 (2017) 48–60, https://doi.org/10.1016/j.partic.2016.11.005.
[8] T. Al-Juwaya, N. Ali, M. Al-Dahhan, Investigation of hydrodynamics of binary solids mixture spouted beds using radioactive particle tracking (RPT) technique, Chem. Eng. Res. Des. 148 (2019) 21–44, https://doi.org/10.1016/j.cherd.2019.05.051.
[9] T. Al-Juwaya, N. Ali, M. Al-Dahhan, Investigation of cross-sectional gas-solid distributions in spouted beds using advanced non-invasive gamma-ray computed tomography (CT), Exp. Therm. Fluid Sci. 86 (2017) 37–53, https://doi.org/10.1016/j.expthermflusci.2017.03.029.
[10] N. Ali, T. Aljuwaya, M. Al-Dahhan, Evaluating the new mechanistic scale-up methodology of gas-solid spouted beds using gamma ray computed tomography (CT), Exp. Therm. Fluid Sci. 104 (2019) 186–198, https://doi.org/10.1016/j.expthermflusci.2019.01.029.
[11] A.J. Sultan, L.S. Sabri, H.S. Majdi, S.K. Jebur, M.H. Al-Dahhan, Study of gas holdup distribution in cylindrical split airlift reactor by using gamma-ray densitometry (GRD), Processes 10 (2022) 910.
[12] C.M. Salgado, W.L. Salgado, R.S.d.F. Dam, C.C. Conti, Calculation of scales in oil pipeline using gamma-ray scattering and artificial intelligence, Measurement 179 (2021), 109455, https://doi.org/10.1016/j.measurement.2021.109455.
[13] A.M. Mayet, T.-C. Chen, S.M. Alizadeh, A.A. Al-Qahtani, A.K. Alanazi, N. A. Ghamry, H.H. Alhashim, E. Eftekhari-Zadeh, Optimizing the gamma ray-based detection system to measure the scale thickness in three-phase flow through oil and petrochemical pipelines in view of stratified regime, Processes 10 (2022), https://doi.org/10.3390/pr10091866.
[14] M.K. Al Mesfer, A.J. Sultan, M.H. Al-Dahhan, Study the effect of dense internals on the liquid velocity field and turbulent parameters in bubble column for Fischer–Tropsch (FT) synthesis by using Radioactive Particle Tracking (RPT) technique, Chem. Eng. Sci. 161 (2017) 228–248, https://doi.org/10.1016/j.ces.2016.12.001.
[15] J. Alvaré, M.H. Al-Dahhan, Liquid phase mixing in trayed bubble column reactors, Chem. Eng. Sci. 61 (2006) 1819–1835, https://doi.org/10.1016/j.ces.2005.10.015.
[16] A.J. Sultan, L.S. Sabri, M.H. Al-Dahhan, Influence of the size of heat exchanging internals on the gas holdup distribution in a bubble column using gamma-ray

computed tomography, Chem. Eng. Sci. 186 (2018) 1–25, https://doi.org/10.1016/j.ces.2018.04.021.
[17] J. Chen, A. Kemoun, M.H. Al-Dahhan, M.P. Duduković, D.J. Lee, L.-S. Fan, Comparative hydrodynamics study in a bubble column using computer-automated radioactive particle tracking (CARPT)/computed tomography (CT) and particle image velocimetry (PIV), Chem. Eng. Sci. 54 (1999) 2199–2207, https://doi.org/10.1016/S0009-2509(98)00349-2.
[18] N. Rados, A. Shaikh, M.H. Al-Dahhan, Solids flow mapping in a high pressure slurry bubble column, Chem. Eng. Sci. 60 (2005) 6067–6072, https://doi.org/10.1016/j.ces.2005.04.087.
[19] J. Chen, N. Rados, M.H. Al-Dahhan, M.P. Duduković, D. Nguyen, K. Parimi, Particle motion in packed/ebullated beds by CT and CARPT, AIChE J. 47 (2001) 994–1004, https://doi.org/10.1002/aic.690470506.
[20] S. Roy, J. Chen, S.B. Kumar, M.H. Al-Dahhan, M.P. Duduković, Tomographic and particle tracking studies in a Liquid−Solid riser, Ind. Eng. Chem. Res. 36 (1997) 4666–4669, https://doi.org/10.1021/ie970292l.
[21] A. Efhaima, M.H. Al-Dahhan, Assessment of scale-up dimensionless groups methodology of gas-solid fluidized beds using advanced non-invasive measurement techniques (CT and RPT), Can. J. Chem. Eng. 95 (2017) 656–669, https://doi.org/10.1002/cjce.22745.
[22] A.R. Rammohan, A. Kemoun, M.H. Al-Dahhan, M.P. Dudukovic, Characterization of single phase flows in stirred tanks via computer automated radioactive particle tracking (CARPT), Chem. Eng. Res. Des. 79 (2001) 831–844, https://doi.org/10.1205/02638760152721343.
[23] A.R. Rammohan, A. Kemoun, M.H. Al-Dahhan, M.P. Dudukovic, A Lagrangian description of flows in stirred tanks via computer-automated radioactive particle tracking (CARPT), Chem. Eng. Sci. 56 (2001) 2629–2639, https://doi.org/10.1016/S0009-2509(00)00537-6.
[24] H.-P. Luo, A. Kemoun, M.H. Al-Dahhan, J.M.F. Sevilla, J.L.G.a. Sánchez, F.G. a. Camacho, E.M. Grima, Analysis of photobioreactors for culturing high-value microalgae and cyanobacteria via an advanced diagnostic technique: CARPT, Chem. Eng. Sci. 58 (2003) 2519–2527, https://doi.org/10.1016/S0009-2509(03)00098-8.
[25] L.S. Sabri, A.J. Sultan, M.H. Al-Dahhan, Split internal-loop photobioreactor for Scenedesmus sp. microalgae: culturing and hydrodynamics, Chin. J. Chem. Eng. 33 (2021) 236–248, https://doi.org/10.1016/j.cjche.2020.07.058.
[26] L.S. Sabri, A.J. Sultan, M.H. Al-Dahhan, Mapping of microalgae culturing via radioactive particle tracking, Chem. Eng. Sci. 192 (2018) 739–758, https://doi.org/10.1016/j.ces.2018.08.012.
[27] L.S. Sabri, A.J. Sultan, H.S. Majdi, S.K. Jebur, M.H. Al-Dahhan, A detailed hydrodynamic study of the split-plate airlift reactor by using non-invasive gamma-ray techniques, ChemEngineering 6 (2022) 18.
[28] M.S. Vesvikar, M. Al-Dahhan, Hydrodynamics investigation of laboratory-scale Internal Gas-lift loop anaerobic digester using non-invasive CAPRT technique, Biomass Bioenergy 84 (2016) 98–106, https://doi.org/10.1016/j.biombioe.2015.11.014.
[29] M.S. Vesvikar, R. Varma, K. Karim, M. Al-Dahhan, Flow pattern visualization in a mimic anaerobic digester: experimental and computational studies, Water Sci. Technol. : a journal of the International Association on Water Pollution Research 52 (2005) 537–543.
[30] W. Du, J. Zhang, S. Bao, J. Xu, L. Zhang, Numerical investigation of particle mixing and segregation in spouted beds with binary mixtures of particles, Powder Technol. 301 (2016) 1159–1171, https://doi.org/10.1016/j.powtec.2016.07.071.
[31] K.G. Santos, M.C.C. Francisquetti, R.A. Malagoni, M.A.S. Barrozo, Fluid dynamic behavior in a spouted bed with binary mixtures differing in size, Dry. Technol. 33 (2015) 1746–1757, https://doi.org/10.1080/07373937.2015.1036284.
[32] R.K. Upadhyay, S. Roy, Investigation of hydrodynamics of binary fluidized beds via radioactive particle tracking and dual-source densitometry, Can. J. Chem. Eng. 88 (2010) 601–610, https://doi.org/10.1002/cjce.20334.
[33] L. Huilin, H. Yurong, D. Gidaspow, Y. Lidan, Q. Yukun, Size segregation of binary mixture of solids in bubbling fluidized beds, Powder Technol. 134 (2003) 86–97, https://doi.org/10.1016/S0032-5910(03)00126-8.
[34] L. Huilin, H. Yurong, D. Gidaspow, Hydrodynamic modelling of binary mixture in a gas bubbling fluidized bed using the kinetic theory of granular flow, Chem. Eng. Sci. 58 (2003) 1197–1205, https://doi.org/10.1016/S0009-2509(02)00635-8.
[35] J.S. Lin, M.M. Chen, B.T. Chao, A novel radioactive particle tracking facility for measurement of solids motion in gas fluidized beds, AIChE J. 31 (1985) 465–473, https://doi.org/10.1002/aic.690310314.
[36] F. Larachi, G. Kennedy, J. Chaouki, A γ-ray detection system for 3-D particle tracking in multiphase reactors, Nucl. Instrum. Methods Phys. Res. Sect. A Accel. Spectrom. Detect. Assoc. Equip. 338 (1994) 568–576, https://doi.org/10.1016/0168-9002(94)91343-9.
[37] S. Roy, F. Larachi, M.H. Al-Dahhan, M.P. Duduković, Optimal design of radioactive particle tracking experiments for flow mapping in opaque multiphase reactors, Appl. Radiat. Isot. 56 (2002) 485–503, https://doi.org/10.1016/S0969-8043(01)00142-7.
[38] S. Bhusarapu, M. Al-Dahhan, M.P. Dudukovic, Quantification of solids flow in a gas–solid riser: single radioactive particle tracking, Chem. Eng. Sci. 59 (2004) 5381–5386, https://doi.org/10.1016/j.ces.2004.07.052.
[39] V. Mosorov, J. Abdullah, MCNP5 code in radioactive particle tracking, Appl. Radiat. Isot. 69 (2011) 1287–1293, https://doi.org/10.1016/j.apradiso.2011.04.028.
[40] O. Dubé, D. Dubé, J. Chaouki, F. Bertrand, Optimization of detector positioning in the radioactive particle tracking technique, Appl. Radiat. Isot. 89 (2014) 109–124, https://doi.org/10.1016/j.apradiso.2014.02.019.
[41] M.A.S.M. Yunos, S.A. Hussain, H.M. Yusoff, J. Abdullah, Preparation and quantification of radioactive particles for tracking hydrodynamic behavior in multiphase reactors, Appl. Radiat. Isot. 91 (2014) 57–61, https://doi.org/10.1016/j.apradiso.2014.05.015.
[42] V. Mosorov, Strategy for fitting source strength and reconstruction procedure in radioactive particle tracking, Appl. Radiat. Isot. 103 (2015) 65–71, https://doi.org/10.1016/j.apradiso.2015.06.007.
[43] M. Rasouli, F. Bertrand, J. Chaouki, A multiple radioactive particle tracking technique to investigate particulate flows, AIChE J. 61 (2015) 384–394, https://doi.org/10.1002/aic.14644.
[44] M.A.S. Mohd Yunos, S.M. Sipaun, S.A. Hussain, Feasibility of using radioactive particle tracking as an alternative technique for experimental investigation in bubble column reactor, IOP Conf. Ser. Mater. Sci. Eng. 554 (2019), 012005, https://doi.org/10.1088/1757-899x/554/1/012005.
[45] J. Biswal, S. Goswami, R.K. Upadhyay, H.J. Pant, Methods of preparation of microparticles for radioactive particle tracking experiments, Appl. Radiat. Isot. (2020), 109380, https://doi.org/10.1016/j.apradiso.2020.109380.
[46] A.A. Alghamdi, T.M. Aljuwaya, A.S. Alomari, M.H. Al-Dahhan, GEANT4 simulation for radioactive particle tracking (RPT) technique, Sensors 22 (2022) 1223.
[47] G. Lindner, S. Shi, S. Vučetić, S. Mišković, Transfer learning for radioactive particle tracking, Chem. Eng. Sci. 248 (2022), 117190, https://doi.org/10.1016/j.ces.2021.117190.
[48] G.A. Lindner, S. Mišković, GIPPE-RPT: geant4 interface for particle physics experiments applied to Radioactive Particle Tracking, Appl. Radiat. Isot. 180 (2022), 110041, https://doi.org/10.1016/j.apradiso.2021.110041.
[49] M.S. Vesvikar, UNDERSTANDING THE HYDRODYNAMICS AND PERFORMANCE OF ANAEROBIC DIGESTERS, Dissertation, WASHINGTON UNIVERSITY, Saint Louis, Missouri, 2006.
[50] Y. Wang, CRC Handbook of Radioactive Nuclides, Chemical Rubber Co., Cleveland (Ohio), 1969.
[51] L.S. Sabri, A.J. Sultan, M.H. Al-Dahhan, Assessment of RPT calibration need during microalgae culturing and other biochemical processes, in: Proceedings of the 2017 International Conference on Environmental Impacts of the Oil and Gas Industries: Kurdistan Region of Iraq as a Case Study (EIOGI), 17-19 April 2017, 2017, pp. 59–64.
[52] S. Bhusarapu, M.H. Al-Dahhan, M.P. Duduković, Solids flow mapping in a gas–solid riser: mean holdup and velocity fields, Powder Technol. 163 (2006) 98–123, https://doi.org/10.1016/j.powtec.2006.01.013.